

# Kinetic Protection of a Water-Soluble Olefin Metathesis Catalyst for Potential Use under Biological Conditions

Catriona C. James,<sup>[a]</sup> Petrus C. M. Laan,<sup>[a]</sup> Bas de Bruin,<sup>[a]</sup> and Joost N. H. Reek<sup>\*,[a]</sup>

Olefin metathesis catalysts like AquaMet are vulnerable to different decomposition pathways under biologically relevant conditions. Currently, stabilizing strategies are focused on approaches with limited relevance for application under biologically relevant conditions. Initial attempts to stabilise AquaMet by encapsulation within a supramolecular metallocage showed that the nitrate counterions of the cage improve the activity of the catalyst. We show that the chloride ligands of AquaMet can be replaced with nitrates by simple anion-

exchange. Catalytic studies into metathesis of a diallyl substrate showed that the presence of nitrate generates higher yields of the ring-closed product compared to AquaMet alone, under aqueous and biological conditions. Kinetic studies support that the nitrate-containing catalyst both initiates faster and performs catalysis at a much faster rate than AquaMet, while the rate of catalyst deactivation was similar. This new strategy of kinetic protection of a transition metal catalyst may have future applications for other catalytic reactions applied *in vivo*.

## Introduction

Ruthenium catalysed olefin metathesis is an extraordinarily useful transformation in organic synthesis,<sup>[1]</sup> providing access to a wide range of products, including ring structures and heterocycles,<sup>[2]</sup> functionalised olefins,<sup>[3]</sup> and polymers.<sup>[4]</sup> The versatility of this transformation has led to its application in a variety of areas, for example the total synthesis of bioactive organic compounds,<sup>[5]</sup> and in the production of pharmaceuticals.<sup>[6]</sup> Importantly, olefin metathesis only requires mild reaction conditions, with many examples running at, or close to, room temperature,<sup>[7]</sup> as well as tolerating the presence of both of water and oxygen.<sup>[8]</sup> Indeed many water-soluble derivatives of classical Hoveyda-Grubbs catalysts have been developed via functionalisation of the NHC backbone with cationic ammonium groups, with varying reactivity and solubility depending on the cation and nature of the ammonium group.<sup>[9]</sup> Therefore it is not surprising that the pursuit of applying the metathesis reaction *in vivo*, for example for *in situ* drug formation or biomolecule labelling, is of current interest.<sup>[10]</sup> Indeed the applicability of this transformation in biological settings has recently been demonstrated with olefin metathesis-mediated labelling of proteins by incorporation of unnatural alkene-containing amino acids into the desired

protein,<sup>[10b,11]</sup> and for the synthesis of small coumarin-based compounds inside cancer cells.<sup>[12]</sup>


The application of catalytic reactions inside living cells is not straight-forward, as the cellular environment poses a substantial threat to the activity of catalysts, as decomposition can readily occur through several deactivation pathways. Cells contain large quantities of metal-binding biomolecules, such as glutathione (GSH), a thiol found in 2–10 mM concentrations in cells,<sup>[13]</sup> and L-histidine (His), an imidazole-containing amino acid. Such substances can readily deactivate metal catalysts by **strong coordination to the metal centre, resulting in low catalytic activity**. As a result, most catalysts applied under biological relevant conditions are typically applied in close to stoichiometric amounts.<sup>[10a,14]</sup>

Despite these challenges, olefin metathesis has been successfully carried out inside living cells. The two reported examples making use of artificial metalloenzymes to protect the catalyst from the poisoning environment of the cell. Ward and co-workers recently presented olefin metathesis in *E. coli* bacteria by docking a Hoveyda-Grubbs derived catalyst inside streptavidin.<sup>[12a]</sup> In this example, catalyst poisoning was avoided by targeting the periplasm of the bacteria, where much lower concentrations of the **metal-binding (and reducing) agent glutathione** are present compared to the interior of the cell. A similar catalyst was also shown to be protected from thiol poisoning by docking it within the hydrophobic pocket of serum albumin, allowing for the generation of a cytotoxic compound within the cytoplasm of cancer cells.<sup>[12b]</sup>

While artificial metalloenzymes provide a route to provide protection against biomolecule binding, there are many other inhibiting components within a cellular environment to which the catalysts are vulnerable. The cytoplasm of cells is an aqueous environment, and at low catalyst loadings (which are required for catalysis in living cells), ruthenium based olefin metathesis catalysts are highly sensitive to the presence of even low quantities of water.<sup>[15]</sup> The rate of catalyst initiation is lowered,<sup>[16]</sup> and the chloride ligands readily dissociate from the

[a] Dr. C. C. James, P. C. M. Laan, Prof. Dr. B. de Bruin, Prof. Dr. J. N. H. Reek  
Van't Hoff Institute for Molecular Sciences  
University of Amsterdam  
Science Park 904  
1098 XH Amsterdam (Netherlands)  
E-mail: j.n.h.reek@uva.nl

 Supporting information for this article is available on the WWW under <https://doi.org/10.1002/cctc.202201272>

 © 2023 The Authors. ChemCatChem published by Wiley-VCH GmbH. This is an open access article under the terms of the Creative Commons Attribution Non-Commercial License, which permits use, distribution and reproduction in any medium, provided the original work is properly cited and is not used for commercial purposes.

ruthenium centre,<sup>[17]</sup> followed by coordination of hydroxide ions to generate  $\text{Ru}(\text{OH})_n$  species, which are completely inactive in metathesis and rapidly decompose via loss of the carbene ligand.<sup>[18]</sup> Moreover, during the catalytic cycle a base-sensitive metallocyclobutane intermediate is formed. Therefore the presence of basic biomolecules may result in deprotonation of this cyclic intermediate, resulting in decomposition of the intermediate and subsequent formation of a species which is not active in metathesis.<sup>[18d,19]</sup> Finally, metathesis catalysts are also susceptible to bimolecular decomposition pathways involving dimerization of the ruthenium centres.<sup>[20]</sup>

There have been several strategies employed to overcome these problems, by improving the stability of the catalyst. The rate of decomposition can be reduced by addition of Brønsted acids to remove hydroxide ions from solution,<sup>[21]</sup> or by addition of chloride salts to prevent the chloride displacement.<sup>[22]</sup> It has also been shown that cationic metathesis catalysts can be protected by encapsulating the complex inside a supramolecular host.<sup>[23]</sup> Encapsulating the catalyst within the cavity of a supramolecular cage separates the catalyst from the surrounding solvent and also prevents catalyst degradation by bimolecular pathways. However, this approach has so far been limited to organic solvent, due to the solubility of the supramolecular capsule which was used. To the best of our knowledge, an olefin metathesis catalyst has never been protected from an aqueous environment by encapsulation within a water-soluble supramolecular host. In addition, water-soluble supramolecular cages are also known to provide protection from biomolecules under biological conditions, by providing a protective barrier between the catalyst and the biomolecules and reducing their interaction with the metal centre.<sup>[24]</sup> We therefore looked to design an alternative strategy to protect an olefin metathesis catalyst from both water-induced decomposition and from biomolecule poisoning using a water-soluble supramolecular cage, in order to improve its reactivity under biological conditions.

## Results and Discussion

### Protection Strategy

We initially attempted to protect apolar olefin metathesis catalysts (Grubbs 1, Grubbs 2, Grubbs 3, and Hoveyda-Grubbs 2) by encapsulation within the hydrophobic cavity of a water-soluble supramolecular cage. To this purpose, we selected the octahedral  $[\text{Pt}_6\text{L}_4](\text{NO}_3)_{12}$  metallocage as additive for a ring-closing metathesis (RCM) reaction (Figure 1). Next to being water-soluble, this cage is also known to encapsulate apolar organic compounds and metal complexes as guests.<sup>[25]</sup> The platinum analogue of this cage was selected because of its greater kinetic stability and robustness compared to its palladium counterpart.<sup>[26]</sup> As encapsulation studies revealed that it was not possible for these apolar catalysts to reside within the cavity of the cage (see S.I.), we then set out to investigate the effect of the cage on a water-soluble analogue of the Hoveyda-Grubbs 2 catalyst, AquaMet (AM). We initially

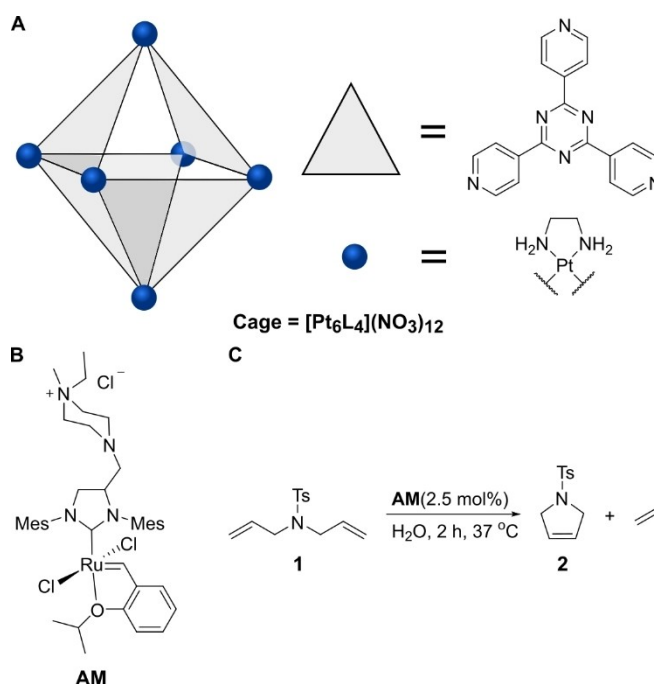


**Figure 1.** A) Structure of the  $[\text{Pt}_6\text{L}_4](\text{NO}_3)_{12}$  cage. B) Structure of AM. C) RCM of substrate 1 to generate ring-closed product 2.

hypothesised that charge repulsion between the cationic ammonium group on the NHC ligand of the catalyst and the cationic platinum centres may reduce the affinity of the catalyst for the cage. However, partial encapsulation of the complex, with the apolar ruthenium centre residing in the hydrophobic cavity and the cationic ammonium group remaining outside by penetrating the large windows of the cage, should be possible. Modelling with GFN2-xTB<sup>[27]</sup> indicated that there would be enough space within the cavity of the cage for such an interaction to occur (Figure S14). The metathesis activity of AM in the both the absence and presence of cage was therefore investigated. Encapsulated complexes often exhibit different activity compared to the free unbound analogue in solution, and therefore a difference in yield could indicate that the cage is interacting with the catalyst in some way. To explore this the ring-closing metathesis of *N,N*-diallyl-tosyl amine, 1, was selected as a model reaction (Table 1). When 2.5 mol% of AM was combined with substrate 1 under aqueous conditions at 37 °C for 2 h, an 18% yield of ring-closed product 2 was achieved. This low yield is likely due to rapid decomposition of the

**Table 1.** Yield of RCM of substrate 1 in the presence of additives.<sup>[a]</sup>

| Entry | Additive       | Yield 1 [%] |
|-------|----------------|-------------|
| 1     | none           | 18 ± 1.5    |
| 2     | cage           | 69 ± 3.8    |
| 3     | $\text{KNO}_3$ | 76 ± 3.2    |

[a] Conditions: 50 mM substrate 1, 2.5 mol% AM, 2.5 mol% cage, 30 mol%  $\text{KNO}_3$ ,  $\text{H}_2\text{O}$ , 37 °C, 2 h. Yield are an average of 3 experiments, and are determined by  $^1\text{H}$  NMR spectroscopy relative 1,3,5-trimethoxybenzene as internal standard (error 5%).

catalyst in water. However, when **AM** was mixed with 1 eq of cage before addition of substrate, a drastic improvement in yield was observed, whereby a 69% yield of **2** was observed. Thus, the presence of the cage during catalysis had a clear, positive influence on the yield of **2**. In order to investigate the origin of this improvement in yield (see S.I. for full details), several control experiments were performed that indicated that it was not the cage itself but the counterions of the cage that was important. Indeed, a control reaction in the presence of 12 eq  $\text{KNO}_3$  with respect to catalyst provided improved yields; 76% yield of **2** was observed compared to 18% yield in absence of this salt. Therefore, it appears that **the presence of nitrate anions greatly improves the reactivity of AM as catalyst for the RCM of substrate 1.**

### Formation of the Nitrate Catalyst

We hypothesised that the origin of the improved activity in the presence of  $\text{KNO}_3$  could be due to binding of nitrate to the ruthenium centre, perhaps by displacing one or both of the chlorides from **AM**, thereby generating a new nitrate catalyst,  $\text{NO}_3\text{-AM}$ . To confirm this, an aqueous solution of **AM** was mixed with an aqueous solution containing an excess of 24 eq of  $\text{KNO}_3$  and analysed by electrospray ionisation high resolution mass spectrometry (ESI-HRMS). Two monocationic ruthenium species containing nitrate were observed (Figure S9 and Figure S10): a peak at 794.3120 which corresponds to the **AM** complex with one of the chlorides replaced by a nitrate,  $[(\text{N}_2\text{C}_8\text{H}_{18}\text{-IMes})(\text{iPrOstyrene})\text{RuCl}(\text{NO}_3)]^+$ ; and a peak at 821.3313 which corresponds to the **AM** complex with no chlorides and two nitrates present,  $[(\text{N}_2\text{C}_8\text{H}_{18}\text{-IMes})(\text{iPrOstyrene})\text{Ru}(\text{NO}_3)_2]^+$ . This shows that when  $\text{NO}_3\text{-AM}$  is generated from **AM** and  $\text{KNO}_3$  a mixture of nitrate-containing species is formed. There are several possibilities to the exact structures of these complexes. It has been shown for nitrate-containing complexes soluble in organic solvents that the nitrate can be bound to the ruthenium centre in either a monodentate<sup>[28]</sup> or bidentate<sup>[29]</sup> fashion, as depicted in Figure 2. It is likely that in both cases the nitrate would be present as a monodentate ligand, as this would result in less steric crowding around the ruthenium centre, although a bidentate nitrate ligand could also be possible (Figure 2). **In the absence of substrate, rapid decomposition of the complex in aqueous solution** upon the addition

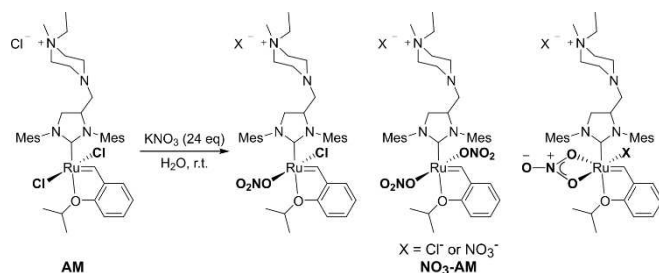


**Figure 2.** Possible structures of the  $\text{NO}_3\text{-AM}$  structures observed with HR-MS after addition of 24 eq of  $\text{KNO}_3$  to **AM**.

of  $\text{KNO}_3$  to **AM** occurs, resulting in the formation of insoluble brown precipitates, meaning full characterisation by NMR spectroscopy was not possible. Therefore, it was not possible to isolate the  $\text{NO}_3\text{-AM}$  complex in order to determine the exact structure of the catalyst.

As the  $\text{NO}_3\text{-AM}$  catalyst cannot be isolated, it needs to be generated *in situ* by mixing  $\text{KNO}_3$  with **AM** just before the start of the catalysis. Therefore, we investigated the optimum amount of nitrate to add in order to obtain the largest improvement in yield of product **2** (Figure 3). To this end, the ring closing metathesis of substrate **1** was carried out in the presence of 2–160 eq. of  $\text{KNO}_3$  with respect to **AM** under aqueous conditions. The addition of 24 eq. of  $\text{KNO}_3$  gave a total yield of 83% of product **2**. Increasing the equivalents of nitrate salt beyond this value did not substantially increase the yield further. Therefore, all further studies were carried out with 24 eq. of nitrate with respect to **AM**. These optimised conditions gave a greater improvement in yield than previously reported methods, and could also be successfully applied to another water-soluble catalyst (see S.I. for full details). Other substrates of varying solubility and structure were also explored to see if the yield of other reactions could be improved by the addition of  $\text{KNO}_3$  in a similar way as for substrate **1**. However, it was found that **for other substrates, both apolar and water-soluble, that nitrate had either negligible or negative effects** (see section *Solubility Studies* in the S.I. for full details and discussion). Based on these data it appears that the increased yield for substrate **1** cannot be explained by solubility reasons alone, but is instead most likely due to a combination of different factors. Therefore, further studies were performed with substrate **1**.

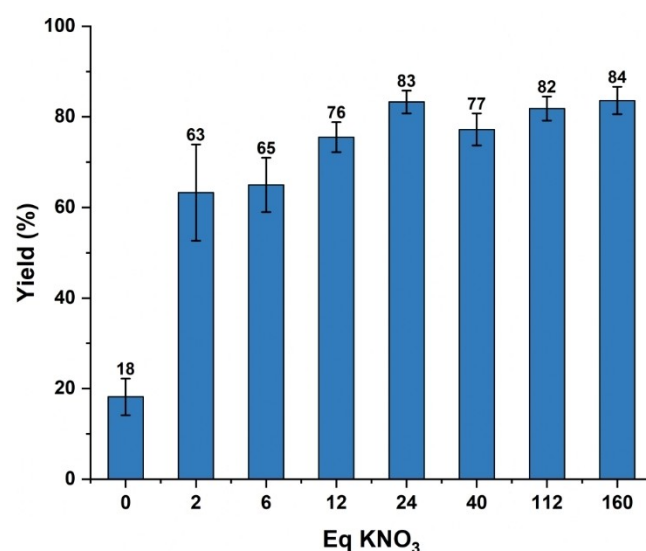


**Figure 3.** Yield of ring closed product **2** with increasing equivalents of  $\text{KNO}_3$  with respect to **AM**. Conditions: 2.5 mol% **AM**,  $\text{KNO}_3$  (x equivalents with respect to **AM**), 50 mM substrate **1**,  $\text{H}_2\text{O}$ , 37 °C, 2 h. Yields are an average of 3 experiments, and are determined by  $^1\text{H}$  NMR spectroscopy relative to 1,3,5-trimethoxybenzene as internal standard (error 5%).

## Kinetic Studies

In order to gain insight into the origin of the improved reactivity of **NO<sub>3</sub>-AM** compared to **AM**, the kinetics of the reaction were monitored. We hypothesised that there are several possibilities as to the origin of these superior yields. It is known that **AM** is highly vulnerable to various decomposition pathways in the presence of water, so therefore it is possible that the catalytically active nitrate complex formed is simply more stable in water than its chloride analogue. This would make the **NO<sub>3</sub>-AM** catalyst less susceptible to decomposition and therefore it would result in a higher concentration of active catalyst in solution. What is also important to consider is that **NO<sub>3</sub>-AM** and **AM** are pre-catalysts: in both cases the isopropoxystyrene ligand must first be replaced by a substrate molecule to enter the catalytic cycle.<sup>[30]</sup> For Hoveyda-Grubbs 2<sup>nd</sup> generation catalysts the first step of this initiation can either be a dissociative or interchange mechanism, depending on the structure of the catalyst and substituents on the isopropoxystyrene ligand.<sup>[31]</sup> Therefore, another possible reason for the better reactivity is that **NO<sub>3</sub>-AM** is able to initiate faster. Faster

initiation would mean that the active species is generated more quickly during the reaction, meaning that more catalytic cycles can take place before the complex is decomposed by the aqueous environment compared to a slower initiating catalyst over the same time frame. While the initiation of **NO<sub>3</sub>-AM** may be different due to structural differences compared to **AM**, it should also be noted that in this heterogenous system a difference in initiation could also be due to solvent effects. Unsubstituted isopropoxystyrene ligands are known to undergo the so-called 'boomerang' mechanism and recombine with the ruthenium centre after catalysis,<sup>[32]</sup> and the presence of nitrate could also be influencing the behaviour of the isopropoxystyrene ligand in this respect. Alternatively, **NO<sub>3</sub>-AM** may simply be a more active catalyst than its chloride counterpart, which effectively means that it produces more product if the decomposition rates are the same.

In order to gain insight into the comparative stability of **NO<sub>3</sub>-AM** and **AM**, the fate of the pre-catalysts was monitored by UV/Vis spectroscopy over time (Figure 4). The decomposition of metathesis catalysts can be monitored by following the decrease in absorption of the MLCT band in the visible

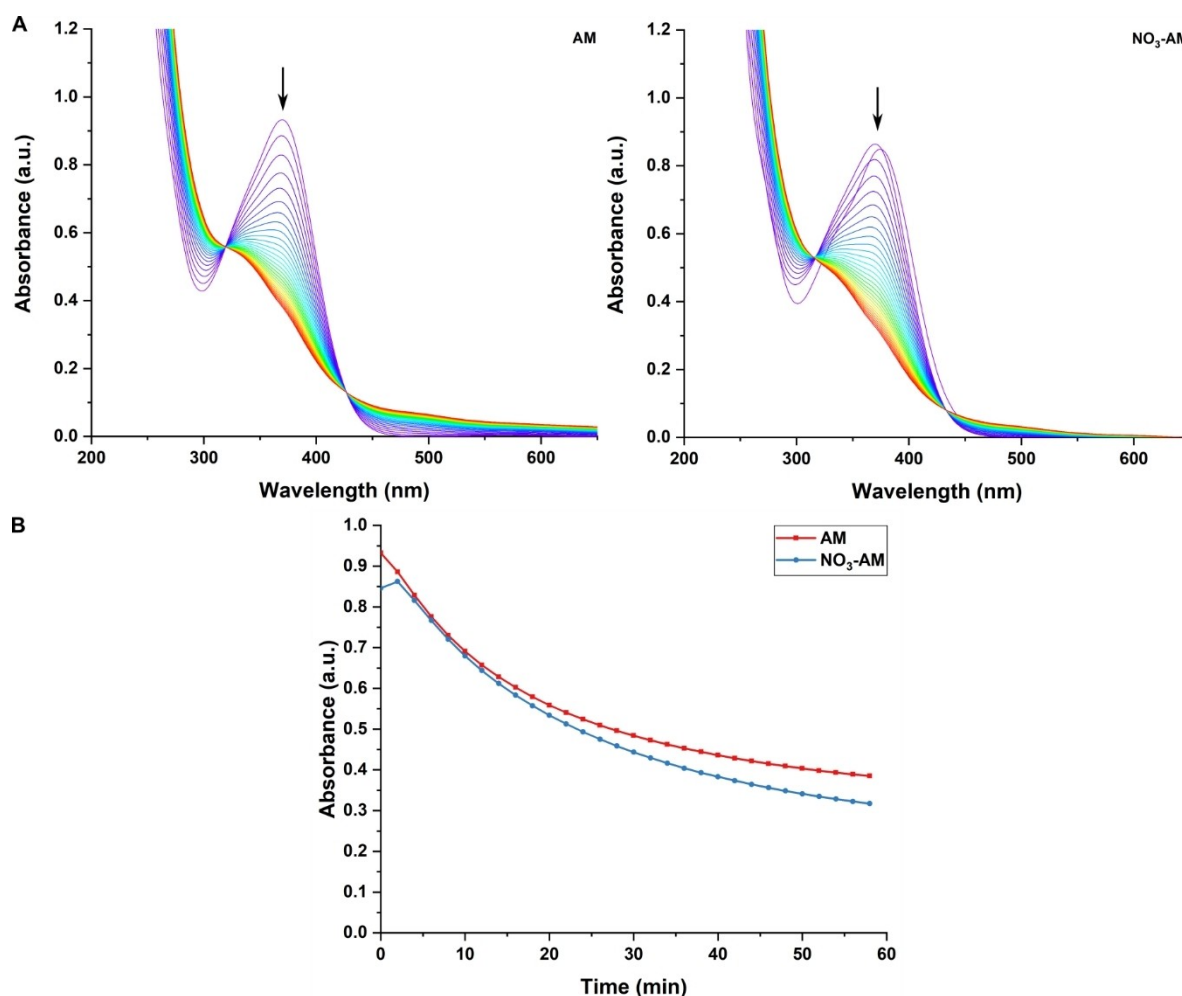


**Figure 4.** A) UV/Vis spectra of **AM** and **NO<sub>3</sub>-AM** pre-catalysts in H<sub>2</sub>O at 37 °C over 1 h. B) Change in absorbance at 370 nm for **AM** and **NO<sub>3</sub>-AM** in H<sub>2</sub>O at 37 °C over 1 h.



region,<sup>[33]</sup> for **AM** this band is found at 370 nm. When left in aqueous solution for 1 h at 37 °C, a steady decrease in the intensity of this peak is observed, from an absorbance of 0.93 down to 0.38, which was accompanied by two sharp isosbestic points at 319 and 427 nm. When **NO<sub>3</sub>-AM** was subjected to the same conditions, the MLCT band in the first spectrum recorded was shifted compared to **AM**, with absorption at 376 nm. However, in the second spectrum measured 2 minutes later, and in all subsequent spectra, this peak was shifted to 370 nm, the same wavelength observed as for **AM**, and again a similar decrease in absorption at this wavelength from 0.85 to 0.31 was accompanied with the appearance of sharp isosbestic points at 319 and 427 nm. Therefore, it appears that **NO<sub>3</sub>-AM** is readily decomposed in the presence of water to give the same decomposition product as **AM**. This indicates that the stability of the pre-catalyst towards decomposition is largely unaffected by the nature of the anionic ligand, as both the nitrate and chloride complexes resulted in similar decomposition rate profiles.

Having established that the pre-catalysts exhibit similar stabilities, the behaviour of the active species under catalytic conditions was then investigated. Insight into the active species can be obtained by UV/Vis spectroscopy, as the decrease in absorption of the MLCT band also corresponds to initiation of the pre-catalyst, as well to decomposition.<sup>[33]</sup> The catalysts were mixed with substrate **1** under aqueous conditions and stirred at 37 °C, with samples measured every 5 min (Figure S7). The decrease in absorption of the MLCT band at 372 nm for **NO<sub>3</sub>-AM** was much steeper than for **AM**: the absorption for **NO<sub>3</sub>-AM** decreased from 1.18 to 0.35 after a total reaction time of 1 h; however, the absorption for **AM** only decreased from 1.21 to 0.51. Since both the **AM** and **NO<sub>3</sub>-AM** pre-catalysts displayed similar decomposition profiles, the larger decrease in the MLCT band for **NO<sub>3</sub>-AM** under catalytic conditions suggests that the initiation rate of the nitrate complex is higher than that of **AM**. To confirm this hypothesis, the rate of product formation was

determined by quantifying the amount of ethene gas produced using a bubble counter.<sup>[34]</sup> Since one equivalent of ethene is produced for every equivalent of product **2** formed, the number and size of bubbles can be used to determine the amount of ethene produced, which can then be equated to the amount of product formed. The kinetic profiles of the ring closing metathesis of substrate **1** by both **AM** and **NO<sub>3</sub>-AM** were determined under aqueous conditions (Figure 5). In the bubble counter setup, **AM** in the presence of water was able to generate **2** in a 20% yield. A short incubation time of around 3 min was observed, before a maximum turnover frequency (TOF) of 252  $\mu\text{mol ethene mol cat}^{-1} \text{ min}^{-1}$  at 13 min was obtained. In contrast, **NO<sub>3</sub>-AM** generated product **2** almost immediately from the start of the reaction. A 31% final yield of **2** was obtained, with a much higher TOF of 3121  $\mu\text{mol ethene mol cat}^{-1} \text{ min}^{-1}$  achieved after only 1.5 min. The lower yield obtained when the reaction was carried out in the bubble counter compared to the previous reactions was attributed to the larger scale (by factor 11), which was required to meet the detection limit of ethene production by the machine. This difference in yield at larger scale may also be indicative of an important role of heterogeneity in the system. In both cases, the final yield was obtained after 1 h, at which point the catalyst was fully deactivated. This was confirmed as the addition of fresh substrate after 1 h did not lead to more product formation (Figure S4). The short incubation time for **NO<sub>3</sub>-AM** again points to the catalyst being faster at initiating the reaction than **AM**, which is in line with the UV/Vis experiments. The kinetic profile was also determined for an experiment where the **KNO<sub>3</sub>** was added to the reaction 10 minutes after the reaction was started. The TOF increased almost immediately from 213 to 3519  $\mu\text{mol ethene mol cat}^{-1} \text{ min}^{-1}$  upon addition of an aqueous solution of **KNO<sub>3</sub>**, giving a final yield of 45% of product **2** after a total reaction time of 1.5 h. The fact that this rapid improvement in TOF is also observed when **KNO<sub>3</sub>** is added even after the **AM** pre-catalyst has already initiated implies that formation of **NO<sub>3</sub>-**

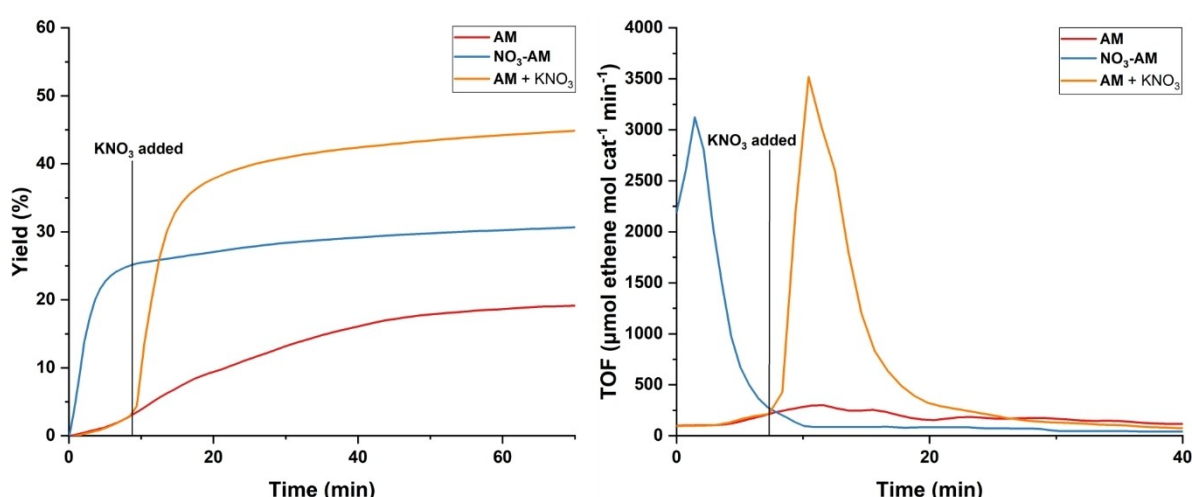


**Figure 5.** Yield and TOF of ring closing metathesis of substrate **1** in the bubble counter under aqueous conditions. Red line: **AM** was used as the catalyst. Blue line: **NO<sub>3</sub>-AM** was used as the catalyst by pre-mixing 24 eq **KNO<sub>3</sub>** with **AM** before addition of substrate **1**. Orange line: **AM** was used as the catalyst, and **KNO<sub>3</sub>** was added approximately 10 min after the start of the reaction. Conditions: 50 mM substrate **1**, 2.5 mol% **AM** or **NO<sub>3</sub>-AM**, 60 mol% **KNO<sub>3</sub>**, **H<sub>2</sub>O**, 37 °C.

AM not only improves the initiation of the catalyst in comparison to AM, but also drastically improves the catalytic activity of the active species.

### Catalysis Under Biological Conditions

We next explored whether this improvement in initiation and catalytic activity could be translated to better performance under biological conditions. Therefore, catalysis was carried out in the presence of metal binding biomolecules. Standard reactions were performed in the presence of a) 1 eq GSH with respect to the catalyst, b) 1 eq His with respect to the catalyst, c) in PBS buffer, and d) 1 eq of GSH and 1 eq of His in PBS buffer. Both the effect on the performance of AM and NO<sub>3</sub>-AM was probed by using substrate 1 (Figure 6). When NO<sub>3</sub>-AM was used as catalyst in the presence of GSH and His, yields of 78% and 67% were obtained respectively. These additives did not substantially decrease the yield compared to the reaction under aqueous conditions (83%). When AM was used as a catalyst a 24% yield was observed in the presence of GSH and a 27% yield in the presence of His. Interestingly, the presence of these additives resulted in an increased yield compared to the reaction under aqueous conditions without additives (18%). Performing the reaction with PBS buffer resulted in a 59% yield when NO<sub>3</sub>-AM was catalyst and an 11% yield when AM was

catalyst. Therefore, PBS buffer had a clear inhibiting affect upon catalysis, regardless of the catalyst used. Since PBS buffer contains a high concentration of chlorides (140 mM), it is expected that chloride competes with the nitrate for binding to the ruthenium centre, and therefore the reduced yield for NO<sub>3</sub>-AM may be due to the fact that generation of the more active nitrate species is less favoured and that a larger proportion of the catalyst remains as its bis-chloride AM form than it does in water. Although the concentration of intracellular chlorides is rather low (around 5 mM), the concentration of extracellular chlorides is around 120 mM, so replacement of the nitrate ligands for chlorides may be a problem during incubation of the catalyst with cells.<sup>[35]</sup> Phosphates are also present in PBS buffer, and these may also induce catalysis inhibition.

Next we investigated the performance of the catalysts in the presence of the biological additives combined, as they are in cells. AM was only able to generate product 2 in a 5% yield in the presence of the mixture of GSH, His and PBS. In contrast, NO<sub>3</sub>-AM in the presence of these inhibitory additives was still able to generate product 2 in a 42% yield. The catalytic efficiency of both AM and NO<sub>3</sub>-AM is greatly reduced under these conditions compared to their reactivity under aqueous conditions. However, the yield obtained when NO<sub>3</sub>-AM was catalyst is a huge improvement in yield not only compared to AM in the presence of biological additives, but also compared to AM under aqueous conditions. Therefore, the fast reaction kinetics achieved by NO<sub>3</sub>-AM allows the catalyst to not only overcome decomposition by water, but also decomposition by biomolecule poisoning.

Next, kinetic studies were carried out in the presence of biological additives in order to confirm that the reason for improved yield in the presence of KNO<sub>3</sub> under biological conditions is also due to enhancement of the reaction rate. The stability of the pre-catalysts in the presence of the biological additives was monitored by UV/Vis spectroscopy. Spectra were recorded over 1 h of aqueous solutions of AM and NO<sub>3</sub>-AM at 37 °C in PBS in the presence of 1 eq of GSH and 1 eq of His with respect to the catalyst (Figure S6). In both cases, in the first spectrum recorded the absorbance of the MLCT bands at 375 and 370 nm, respectively, had already decreased to around 0.2, and thereafter steadily increased in absorption to around 0.3. As was observed for the pre-catalysts in water, the resultant spectra observed were the same for both AM and NO<sub>3</sub>-AM. It is likely that the rapid initial disappearance of the MLCT band was due to immediate biomolecule binding, as the soft ruthenium centre is likely to bind strongly to the soft sulfur atom of GSH. Therefore, the stability of the pre-catalysts was confirmed to not be dependent upon the presence of nitrate in the presence of biological additives, as was the case for the pre-catalysts in water. The behaviour of the complexes under catalytic conditions was then explored in order to determine whether or not catalyst initiation also followed the same trend under biological conditions as under aqueous conditions. The catalysts were mixed with substrate 1 in PBS in the presence of 1 eq GSH and 1 eq His with respect to catalyst and stirred at 37 °C, with samples measured every 5 min by UV/Vis spectroscopy (Figure S8). While for AM the absorption at 370 nm decreased from

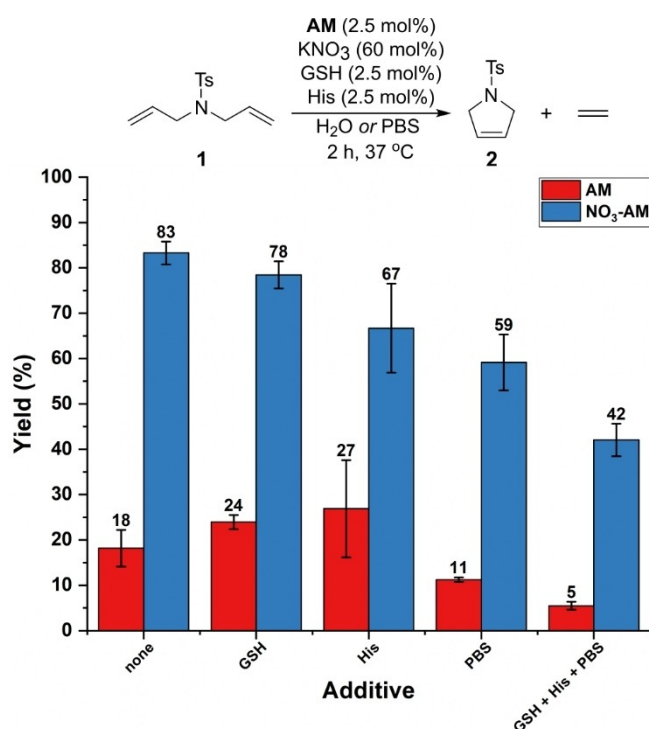


**Figure 6.** Yield of ring closed product 2 by AM (red) or NO<sub>3</sub>-AM (60 mol% KNO<sub>3</sub>, blue) under aqueous conditions (no additive) or in the presence of biological additives. Conditions: 2.5 mol% AM or NO<sub>3</sub>-AM (60 mol% KNO<sub>3</sub>), 50 mM substrate 1, 2.5 mol% GSH, 2.5 mol% His, H<sub>2</sub>O or PBS, 37 °C, 2 h. Yields are an average of 3 experiments, and are determined by <sup>1</sup>H NMR spectroscopy relative to 1,3,5-trimethoxybenzene as internal standard (error 5%).

0.59 to 0.47, the absorption for **NO<sub>3</sub>-AM** decreased from 0.62 to 0.43. Interestingly, the decrease in absorption for both catalysts followed the same profile for the first 25 min, after which **NO<sub>3</sub>-AM** decreased more steeply than **AM**.

The fact that the decomposition rate profiles are the same for both catalysts during this initial timeframe of the reaction, indicates that under biological conditions there may not be a large difference between the catalysts in the rate of initiation. Catalysis was next carried out in the bubble counter to gain better insight into the difference in activity of the active catalysts (Figure S5). Both catalysts were again mixed with 1 eq GSH and 1 eq His with respect to catalyst in a PBS/H<sub>2</sub>O mixture in the presence of substrate **1** at 37 °C. When **AM** was used as a catalyst, after 2 h no gas evolution was observed. At this time the reaction mixture was extracted into toluene-*d*<sub>8</sub> and analysed by <sup>1</sup>H NMR spectroscopy. Only signals corresponding to substrate **1** were observed in the <sup>1</sup>H NMR spectrum, indicating that the presence of biological additives completely prevented the formation of **2**. In contrast, when **NO<sub>3</sub>-AM** was catalyst product **2** was generated in a 12% yield in the presence of biological additives, with a maximum TOF of 797 μmol ethene molcat<sup>-1</sup> min<sup>-1</sup> within the first minute of the reaction. This immediate spike in TOF implies that **NO<sub>3</sub>-AM** is indeed still able to initiate faster under biologically relevant conditions than **AM** in water. The kinetic profile was again determined when KNO<sub>3</sub> was added 10 minutes after the start of the reaction under biological conditions. The TOF immediately increased from 62 to 726 μmol ethene molcat<sup>-1</sup> min<sup>-1</sup> upon addition of KNO<sub>3</sub> and a final yield of 17% of product **2** was obtained after a total reaction time of 1.5 h. The delayed addition of KNO<sub>3</sub> resulted in a rapid increase in activity of the catalyst. Therefore, it appears that under biological conditions the presence of nitrate increases the rate of ring closing metathesis of substrate **1** with **AM** by increasing the activity of the catalyst, and likely also improves the rate of initiation.

## Conclusion

The water-soluble **AM** metathesis catalyst is vulnerable to various decomposition pathways under aqueous conditions. Primarily, water itself results in rapid decomposition of the complex through replacement of the chloride ligand to generate catalytically inactive hydroxide species, and the presence of a mixture of biological additives renders the catalyst almost completely inactive. Although encapsulation of apolar olefin metathesis catalysts within a [Pt<sub>6</sub>L<sub>4</sub>](NO<sub>3</sub>)<sub>12</sub> cage was not a viable strategy for catalyst protection, the addition of nitrate to **AM** results in a dramatic improvement in catalytic activity for the ring closing metathesis of substrate **1**. The ring-closed product **2** is generated in an 83% yield under aqueous conditions, and in a 42% yield even in the presence of a mixture of biological additives. A combination of solubility effects, on-water effects, and of the formation of a new **NO<sub>3</sub>-AM** complex results in much faster reaction kinetics: product formation is faster than decomposition or poisoning, allowing the catalyst to convert more substrate before the catalyst is

deactivated, and in this way the catalyst is protected from biologically relevant conditions. This kinetic protection of the catalyst by addition of KNO<sub>3</sub> is therefore a new, facile and useful route to protecting an aqueous olefin metathesis catalyst under biological conditions. Future work should investigate the scope of this strategy for other metathesis substrates, and whether or not this method of protection is also feasible inside of living cells.

## Experimental Section

### General Catalysis procedure

Stock solutions of KNO<sub>3</sub>, **AM**, GSH, and His in H<sub>2</sub>O were prepared. The desired volume of H<sub>2</sub>O or KNO<sub>3</sub> (18 μmol, 60 mol%) was mixed together with **AM** (0.75 μmol, 2.5 mol%). Then, the desired bioadditive (0.75 μmol, 2.5 mol%) was added, followed by neat substrate **1** (6.8 μL, 7.5 mg, 30 μmol, 1 eq). The vial was capped and stirred at 37 °C for 2 h. 0.8 mL of a 40 mM solution of 1,3,5-trimethoxybenzene in toluene-*d*<sub>8</sub> was added, and the vial was shaken. The organic layer was decanted to an NMR tube and measured. The yields of the product were determined by <sup>1</sup>H NMR spectroscopy relative to 1,3,5-trimethoxybenzene as internal standard.

## Acknowledgements

We would like to thank Ed Zuidinga for ESI-HRMS measurements.

## Conflict of Interest

The authors declare no conflict of interest.

## Data Availability Statement

The data that support the findings of this study are available from the corresponding author upon reasonable request.

**Keywords:** homogeneous catalysis · bioinorganic chemistry · metathesis · kinetics

- [1] a) R. H. Grubbs, S. Chang, *Tetrahedron* **1998**, *54*, 4413–4450; b) T. M. Trnka, R. H. Grubbs, *Acc. Chem. Res.* **2001**, *34*, 18–29; c) M. R. Becker, R. B. Watson, C. S. Schindler, *Chem. Soc. Rev.* **2018**, *47*, 7867–7881; d) A. H. Hoveyda, A. R. Zhugralin, *Nature* **2007**, *450*, 243–251.
- [2] a) A. Deiters, S. F. Martin, *Chem. Rev.* **2004**, *104*, 2199–2238; b) I. Nakamura, Y. Yamamoto, *Chem. Rev.* **2004**, *104*, 2127–2198; c) S. Kotha, M. Meshram, Y. Dommaraju, *Chem. Rev.* **2018**, *18*, 1613–1632.
- [3] R. H. Grubbs, *Tetrahedron* **2004**, *60*, 7117–7140.
- [4] M. L. Gringolts, Y. I. Denisova, E. S. Finkelshtein, Y. V. Kudryavtsev, *Beilstein J. Org. Chem.* **2019**, *15*, 218–235.
- [5] a) A. Fürstner, *Chem. Commun.* **2011**, *47*, 6505–6511; b) K. C. Nicolaou, P. G. Bulger, D. Sarlah, *Angew. Chem. Int. Ed.* **2005**, *44*, 4490–4527; *Angew. Chem.* **2005**, *117*, 4564–4601; c) H. C. M. a. S. B. William, *Curr. Top. Med. Chem.* **2005**, *5*, 1521–1540.
- [6] a) M. Tyagi, F. Begnini, V. Poongavanam, B. C. Doak, J. Kihlberg, *Chem.–Eur. J.* **2020**, *26*, 49–88; b) A. C. Flick, C. A. Leverett, H. X. Ding, E.

- McInturff, S. J. Fink, C. J. Helal, C. J. O'Donnell, *J. Med. Chem.* **2019**, 62, 7340–7382; c) M. Yu, S. Lou, F. Gonzalez-Bobes, *Org. Process Res. Dev.* **2018**, 22, 918–946; d) C. S. Higman, J. A. M. Lummiss, D. E. Fogg, *Angew. Chem. Int. Ed.* **2016**, 55, 3552–3565; *Angew. Chem.* **2016**, 128, 3612–3626.
- [7] a) D. O. Ponkratov, A. S. Shaplov, Y. S. Vygodskii, *Polym. Sci. Ser. C* **2019**, 61, 2–16; b) D. Bartscher, K. Grela, *Angew. Chem. Int. Ed.* **2009**, 48, 442–454; *Angew. Chem.* **2009**, 121, 450–462; c) J. Tomasek, J. Schatz, *Green Chem.* **2013**, 15, 2317–2338; d) P. A. Thomas, B. B. Marvey, *Molecules* **2016**, 21, 16; e) N. Rios-Lombardia, J. Garcia-Alvarez, J. Gonzalez-Sabin, *Catalysts* **2018**, 8, 28.
- [8] a) L. Piola, F. Nagra, S. P. Nolan, *Beilstein J. Org. Chem.* **2015**, 11, 2038–2056; b) S. J. Ton, D. E. Fogg, *ACS Catal.* **2019**, 9, 11329–11334; c) J. Tomasek, M. Seßler, H. Gröger, J. Schatz, *Molecules* **2015**, 20, 19130–19141; d) B. M. Novak, R. H. Grubbs, *J. Am. Chem. Soc.* **1988**, 110, 7542–7543; e) S. J. Connon, M. Rivard, M. Zaja, S. Blechert, *Adv. Synth. Catal.* **2003**, 345, 572–575; f) A. Michrowska, Ł. Gułajski, Z. Kaczmarzka, K. Mennecke, A. Kirschning, K. A. Grela, *Green Chem.* **2006**, 8, 685–688; g) K. Skowerski, G. Szczepaniak, C. Wierzbicka, Ł. Gułajski, M. Bieniek, K. Grela, *Catal. Sci. Technol.* **2012**, 2, 2424–2427.
- [9] a) T. K. Olszewski, M. Bieniek, K. Skowerski, *Org. Process Res. Dev.* **2020**, 24, 125–145; b) G. Szczepaniak, K. Kosinski, K. Grela, *Green Chem.* **2014**, 16, 4474–4492.
- [10] a) A. H. Ngo, S. Bose, L. H. Do, *Chem.–Eur. J.* **2018**, 24, 10584–10594; b) M. S. Messina, H. D. Maynard, *Mater. Chem. Front.* **2020**, 4, 1040–1051; c) T. Matsuo, *Catalysts* **2021**, 11, 359; d) A. Boto, C. C. González, D. Hernández, I. Romero-Estudillo, C. J. Saavedra, *Org. Chem. Front.* **2021**, 8, 6720–6759.
- [11] a) Y. A. Lin, J. M. Chalker, B. G. Davis, *ChemBioChem* **2009**, 10, 959–969; b) Y. A. Lin, O. Boutureira, L. Lercher, B. Bhushan, R. S. Paton, B. G. Davis, *J. Am. Chem. Soc.* **2013**, 135, 12156–12159; c) J. M. Chalker, Y. A. Lin, O. Boutureira, B. G. Davis, *Chem. Commun.* **2009**, 3714–3716; d) A. Brik, *Adv. Synth. Catal.* **2008**, 350, 1661–1675.
- [12] a) M. Jeschek, R. Reuter, T. Heinisch, C. Trindler, J. Klehr, S. Panke, T. R. Ward, *Nature* **2016**, 537, 661; b) S. Eda, I. Nasibullin, K. Vong, N. Kudo, M. Yoshida, A. Kurbangalieva, K. Tanaka, *Nat. Catal.* **2019**, 2, 780–792.
- [13] H. J. Forman, H. Zhang, A. Rinna, *Mol. Aspects Med.* **2009**, 30, 1–12.
- [14] a) Y. G. Bai, J. F. Chen, S. C. Zimmerman, *Chem. Soc. Rev.* **2018**, 47, 1811–1821; b) S. Alonso-de Castro, A. Terenzi, J. Gurruchaga-Pereda, L. Salassa, *Chem.–Eur. J.* **2019**, 25, 6651–6660; c) S.-Y. Jang, D. P. Murale, A. D. Kim, J.-S. Lee, *ChemBioChem* **2019**, 20, 1498–1507; d) M. Martínez-Calvo, J. L. Mascareñas, *Coord. Chem. Rev.* **2018**, 359, 57–79; e) J. J. Soldevila-Barreda, N. Metzler-Nolte, *Chem. Rev.* **2019**, 119, 829–869.
- [15] a) A. G. Santos, G. A. Bailey, E. N. dos Santos, D. E. Fogg, *ACS Catal.* **2017**, 7, 3181–3189; b) C. O. Blanco, J. Sims, D. L. Nascimento, A. Y. Goudreault, S. N. Steinmann, C. Michel, D. E. Fogg, *ACS Catal.* **2021**, 11, 893–899.
- [16] a) J. C. Foster, S. Varlas, L. D. Blackman, L. A. Arkinstall, R. K. O'Reilly, *Angew. Chem. Int. Ed.* **2018**, 57, 10672–10676; *Angew. Chem.* **2018**, 130, 10832–10836; b) D. M. Lynn, B. Mohr, R. H. Grubbs, *J. Am. Chem. Soc.* **1998**, 120, 1627–1628.
- [17] M. Kim, M.-S. Eum, M. Y. Jin, K.-W. Jun, C. W. Lee, K. A. Kuen, C. H. Kim, C. S. Chin, *J. Organomet. Chem.* **2004**, 689, 3535–3540.
- [18] a) A. Y. Goudreault, D. M. Walden, D. L. Nascimento, A. G. Botti, S. N. Steinmann, C. Michel, D. E. Fogg, *ACS Catal.* **2020**, 10, 3838–3843; b) J. C. Foster, M. C. Grocott, L. A. Arkinstall, S. Varlas, M. J. Redding, S. M. Grayson, R. K. O'Reilly, *J. Am. Chem. Soc.* **2020**, 142, 13878–13885; c) B. Bhushan, Y. A. Lin, M. Bak, A. Phanumartwivath, N. Yang, M. K. Bilyard, T. Tanaka, K. L. Hudson, L. Lercher, M. Stegmann, S. Mohammed, B. G. Davis, *J. Am. Chem. Soc.* **2018**, 140, 14599–14603; d) W. L. McClennan, S. A. Ruff, J. A. M. Lummiss, D. E. Fogg, *J. Am. Chem. Soc.* **2016**, 138, 14668–14677.
- [19] a) B. J. Ireland, B. T. Dobigny, D. E. Fogg, *ACS Catal.* **2015**, 5, 4690–4698; b) D. L. Nascimento, I. Reim, M. Foscato, V. R. Jensen, D. E. Fogg, *ACS Catal.* **2020**, 10, 11623–11633.
- [20] a) D. L. Nascimento, M. Foscato, G. Occhipinti, V. R. Jensen, D. E. Fogg, *J. Am. Chem. Soc.* **2021**, 143, 11072–11079; b) V. Thiel, K.-J. Wannowius, C. Wolff, C. M. Thiele, H. Plenio, *Chem.–Eur. J.* **2013**, 19, 16403–16414; c) G. A. Bailey, M. Foscato, C. S. Higman, C. S. Day, V. R. Jensen, D. E. Fogg, *J. Am. Chem. Soc.* **2018**, 140, 6931–6944; d) D. L. Nascimento, D. E. Fogg, *J. Am. Chem. Soc.* **2019**, 141, 19236–19240.
- [21] D. M. Lynn, B. Mohr, R. H. Grubbs, *J. Am. Chem. Soc.* **1998**, 120, 1627–1628.
- [22] a) J. C. Foster, M. C. Grocott, L. A. Arkinstall, S. Varlas, M. J. Redding, S. M. Grayson, R. K. O'Reilly, *J. Am. Chem. Soc.* **2020**, 142, 13878–13885; b) T. Matsuo, T. Yoshida, A. Fujii, K. Kawahara, S. Hirota, *Organometallics* **2013**, 32, 5313–5319; c) D. C. Church, L. Takiguchi, J. K. Pokorski, *Polym. Chem.* **2020**, 11, 4492–4499.
- [23] L. J. Jongkind, M. Rahimi, D. Poole Iii, S. J. Ton, D. E. Fogg, J. N. H. Reek, *ChemCatChem* **2020**, 12, 4019–4023.
- [24] C. C. James, D. Wu, E. O. Bobylev, A. Kros, B. de Bruin, J. N. H. Reek, *ChemCatChem* **2022**, 14, e202200942.
- [25] a) S. H. A. M. Leenders, R. Becker, T. Kumpulainen, B. de Bruin, T. Sawada, T. Kato, M. Fujita, J. N. H. Reek, *Chem.–Eur. J.* **2016**, 22, 15468–15474; b) M. Yoshizawa, J. K. Klosterman, M. Fujita, *Angew. Chem. Int. Ed.* **2009**, 48, 3418–3438; *Angew. Chem.* **2009**, 121, 3470–3490; c) T. Murase, M. Fujita, *Chem. Rec.* **2010**, 10, 342–347; d) S. Horiuchi, T. Murase, M. Fujita, *J. Am. Chem. Soc.* **2011**, 133, 12445–12447.
- [26] F. Ibukuro, T. Kusukawa, M. Fujita, *J. Am. Chem. Soc.* **1998**, 120, 8561–8562.
- [27] C. Bannwarth, S. Ehlert, S. Grimme, *J. Chem. Theory Comput.* **2019**, 15, 1652–1671.
- [28] a) M. R. Buchmeiser, I. Ahmad, V. Gurram, P. S. Kumar, *Macromolecules* **2011**, 44, 4098–4106; b) M. Jović, S. Torker, P. Chen, *Organometallics* **2011**, 30, 3971–3980.
- [29] a) M. Malinowska, M. Kozłowska, A. Hryniewicka, J. W. Morzycki, *J. Organomet. Chem.* **2019**, 896, 154–161; b) B. K. Keitz, K. Endo, P. R. Patel, M. B. Herbert, R. H. Grubbs, *J. Am. Chem. Soc.* **2012**, 134, 693–699; c) Y. Dang, Z.-X. Wang, X. Wang, *Organometallics* **2012**, 31, 8654–8657; d) M. A. Pribisko, T. S. Ahmed, R. H. Grubbs, *Polyhedron* **2014**, 84, 144–149; e) S. L. Mangold, D. J. O'Leary, R. H. Grubbs, *J. Am. Chem. Soc.* **2014**, 136, 12469–12478.
- [30] a) J. M. Bates, J. A. M. Lummiss, G. A. Bailey, D. E. Fogg, *ACS Catal.* **2014**, 4, 2387–2394; b) M. Bieniek, A. Michrowska, D. L. Usanov, K. Grela, *Chem.–Eur. J.* **2008**, 14, 806–818; c) S. B. Garber, J. S. Kingsbury, B. L. Gray, A. H. Hoveyda, *J. Am. Chem. Soc.* **2000**, 122, 8168–8179; d) J. S. Kingsbury, J. P. A. Harrity, P. J. Bonitatebus, A. H. Hoveyda, *J. Am. Chem. Soc.* **1999**, 121, 791–799.
- [31] a) T. Basak, K. Grudzień, M. Barbasiewicz, *Eur. J. Inorg. Chem.* **2016**, 3513–3523; b) L. Monsigny, J. Piątkowski, D. Trzybiński, K. Woźniak, T. Nienafłowski, A. Kajetanowicz, K. Grela, *Adv. Synth. Catal.* **2021**, 363, 4590; c) K. M. Engle, G. Lu, S.-X. Luo, L. M. Henling, M. K. Takase, P. Liu, K. N. Houk, R. H. Grubbs, *J. Am. Chem. Soc.* **2015**, 137, 17, 5782–5792; d) V. Thiel, M. Hendann, K.-J. Wannowius, H. Plenio, *J. Am. Chem. Soc.* **2012**, 134, 1104–1114.
- [32] a) J. M. Bates, J. A. M. Lummiss, G. A. Bailey, D. E. Fogg, *ACS Catal.* **2014**, 4, 2387–2394; b) M. Bieniek, A. Michrowska, D. L. Usanov, K. Grela, *Chem.–Eur. J.* **2008**, 14, 806–818; c) S. B. Garber, J. S. Kingsbury, B. L. Gray, A. H. Hoveyda, *J. Am. Chem. Soc.* **2000**, 122, 8168–8179; d) J. S. Kingsbury, J. P. A. Harrity, P. J. Bonitatebus, A. H. Hoveyda, *J. Am. Chem. Soc.* **1999**, 121, 791–799.
- [33] N. Peschek, K.-J. Wannowius, H. Plenio, *ACS Catal.* **2019**, 9, 951–959.
- [34] a) T. K. Slot, N. R. Shiju, G. Rothenberg, *Angew. Chem. Int. Ed.* **2019**, 58, 17273–17276; *Angew. Chem.* **2019**, 131, 17433–17436; b) T. K. Slot, N. Riley, N. R. Shiju, J. W. Medlin, G. Rothenberg, *Chem. Sci.* **2020**, 11, 11024–11029.
- [35] A. V. Melikh, M. I. Sutormina, *J. Theor. Biol.* **2008**, 252, 247–254.

Manuscript received: October 21, 2022

Revised manuscript received: February 8, 2023

Accepted manuscript online: February 8, 2023

Version of record online: March 6, 2023



Copyright of ChemCatChem is the property of Wiley-Blackwell and its content may not be copied or emailed to multiple sites or posted to a listserv without the copyright holder's express written permission. However, users may print, download, or email articles for individual use.